Spectral Analysis of Gold-type Pseudo-random Codes in GNSS Systems

Lucjan Setlak, and Rafał Kowalik

***Abstract*—**The pseudo-random codes, including *Gold's* codes, are used in GNSS systems; they are characterized by good synchronization and the simplicity of their generation. However, the disadvantage of these pseudo-random codes is poor asynchronization. With this in mind, an algorithm improving their properties was implemented in the *Gold's* code structure, which translated into their performance in CDMA code multiple access. The article discusses the method of production of *Gold* sequence and presents their basic properties along with the ways of creating pseudo-random codes. Their spectral analysis was carried out on the example of codes transmitted in GALILEO system signals. On the basis of the waveform of individual components included in the *Gold's* sequence, the spectral power density was determined and its properties were discussed. On this basis, it was found that *Gold's* codes are characterized by better frequency performance, increased use of the transmitted signal power and better properties for disturbances resulting from the presence of noise in the AWGN *(Additive White Gaussian Noise)* radio channel. This article was prepared on the basis of studies of correlation properties between the sequence of *Gold's* codes and the usual sequences of pseudo-noise codes. The final part of the paper presents the simulation results obtained in the Matlab/Simulink environment and practical conclusions were formulated.

***Keywords*—**spectral analysis, pseudo-random codes system, technological solutions, Global Navigation Satellite System

I. Introduction

NOWADAYS you can observe dynamic development of navigation systems, including GALILEO and GNSS *(Global Navigation Satellite System)* in terms of the spreading codes used in these systems. They are created from the combination of the so-called *primary* and *secondary* codes. The lengths of these codes are strictly determined and fixed for individual signal components, as illustrated in Table I. Ranging codes (primary) can be pseudo-random sequences, generated using a feedback register or so-called *optimized pseudo-noise sequences* [1], [2].

In the first case, codes are generated on the basis of two M-sequences shortened to the required length; they can be generated on a regular basis in registers or stored in memory. In the second case *(optimized pseudo-noise sequences)* - codes must be stored in memory. The sequences of secondary codes are fixed and determined "rigidly".

TABLE I. Lengths of ranging codes for individual components

Component	The length of the code sequence [ms]	The length of the code sequence [chipy]	
		Primary code	Secondary code
E5a-I	20	10230	20
E5a-Q	100	10230	100
E5b-I	4	10230	4
E5b-Q	100	10230	100
E1-B	4	4092	-
E1-C	100	4092	25

Ranging codes (primary) can be pseudo-random sequences, generated using a feedback register or so-called *optimized pseudo-noise sequences*.

In the first case, codes are generated on the basis of two M-sequences shortened to the required length; they can be generated on a regular basis in registers or stored in memory. In the second case *(optimized pseudo-noise sequences)* - codes must be stored in memory. The sequences of secondary codes are fixed and determined "rigidly" [3], [4], [5].

The figure below (Fig. 1) presents the method of generating code sequences based on basic and secondary codes. Based on the above, it can be observed that these sequences are created according to the *tiered codes* structure, in which the secondary codes are used to modify the next repetitions of the primary code.

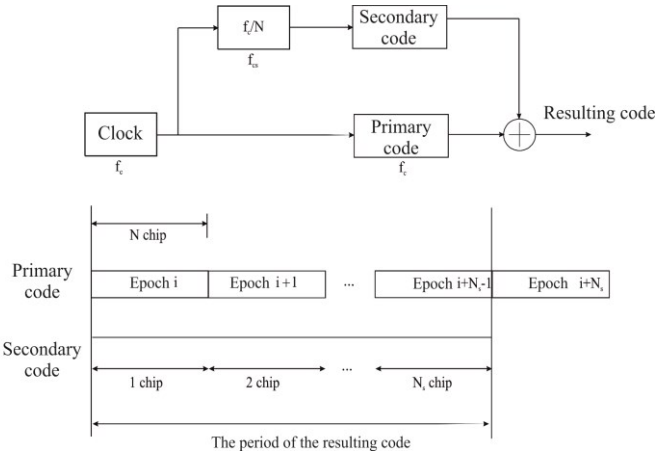

Fig. 1 Primary and secondary PRN code generator in the Galileo system. The following symbols were assumed: N- length of the primary code, N_S- length of the secondary code, f_c- chip rate of the basic code and $f_{cs} = f_c/N$- chip rate of the secondary code.

The general scheme of the register generating sequences of basic code based on the so-called M- sequences is presented in figure above. It should be noted that in order to ensure the desired length of the resulting sequences (N), after N- work

Lucjan Setlak is with the Polish Air Force University, Aviation Division, Department of Avionics and Control System, Deblin, Poland (corresponding author to provide phone: +48-261-518-865, e-mail: l.setlak@law.mil.pl).

Rafał Kowalik is with the Polish Air Force University, Aviation Division, Department of Avionics and Control System, Deblin, Poland (phone: +48-261-518-824, e-mail: r.kowalik@law.mil.pl).

cycles, the content of the two shift registers is reset and initialized with the so-called start values *(start-values)* $\bar{s}_j = [s_j^1, \dots, s_j^R]$ again, where R- is the length of the shift register. For full description of the above register, it is necessary to know the location of its tappings [6], [7].

In the next figure (Fig. 2), the tappings are defined by elements of the vector $\bar{a}_j = [a_{j,1}, a_{j,2}, \dots, a_{j,R-1}, a_{j,R}]$, $a_{j,i} \in \{0,1\}$, of course the zero value $a_{j,i}$- means no connection, and the one - means the occurrence of a tapping in a given place. In documentation, codes (or, to be more precise, registers generating these codes) are most often defined by means of a polynomial description (in octal notation), which can easily be transformed into a vector $\bar{a}_j$, thus obtaining information about the position of subsequent joins in the shift register.

The procedure (algorithm) is as follows: the octal definition of the register should be written in binary form, and then the received bits should be counted from the right side, starting from i = 0, LSB *(Least Significant Bit)* – the least significant bit, and ending with $i = R$, MSB *(Most Significant Bit)* - the most significant bit, where R- is the length of the register.

Then the i-th counted bit represents the i-th element of the vector $a_{j,i}$, for $i = 1, \dots, R$ [8], [9], [10].

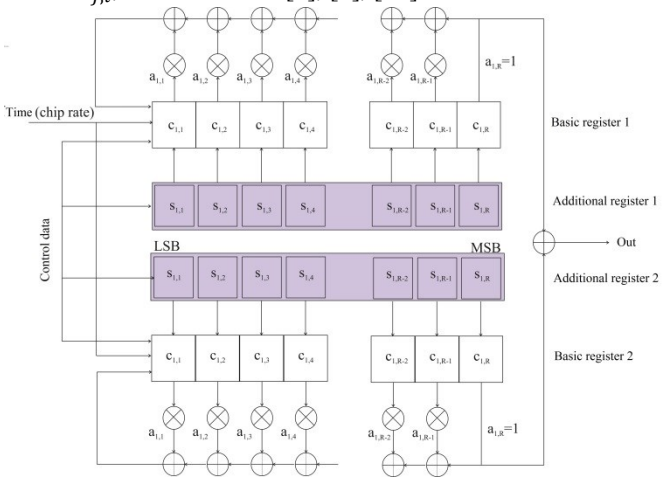

Fig. 2 Operation of pseudorandom sequence registers in the Galileo system

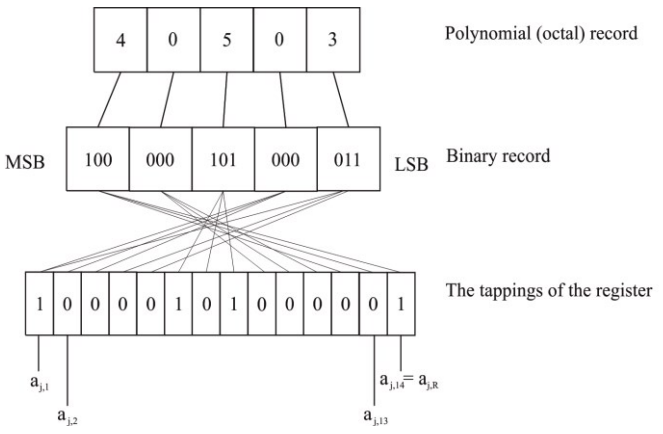

Fig. 3 An example of an octal record transformation defining a shift register into a vector form a_j

It should be emphasized that the bit counting started from zero, assigning bits to the next elements of the vector $a_{j,i}$- however takes place from i = 1. The value $a_{j,R}$ is always equal to one. This process (for an exemplary polynomial value) is shown in the figure below (Fig. 3). A slightly different method of conduct applies in the case of transforming an octal figure of the so-called start values in the corresponding logic levels. To do this, first write the octal record in binary form and then count the bits starting with i = 1 (LSB) up to $i = R$ (MSB), where R- means the length of the register. After this count, the i-th bit corresponds to the element s_j^i of the vector $\bar{s}_j$ [11], [12], [13]. The following is an example of the implementation of the described procedure (Fig. 4).

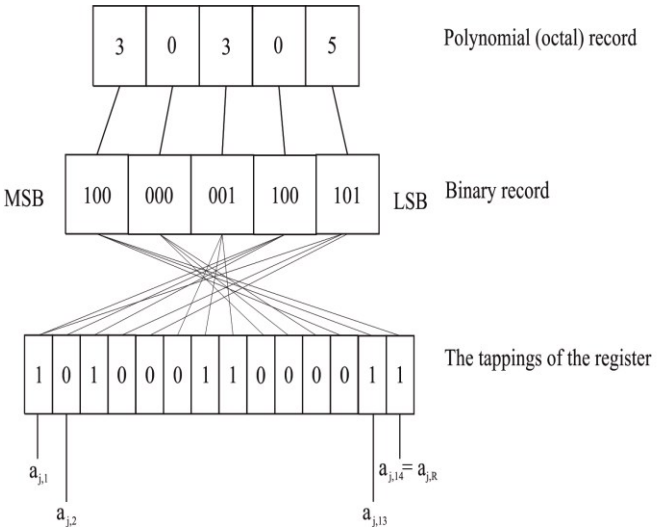

Fig. 4 An example of an octal record transformation of start values to the corresponding logical values

A detailed list of all codes in the GALILEO system can be found in the document [14]. The document contains all the octal polynomials defining the joins, start values as well as the list of secondary codes. It should be added that the assignment of specific numbers of primary and secondary codes to specific satellites is not yet decided. This may be supplemented with the next system specification update.

II. Analysis of the Problem of Spreading the Signal Spectrum in the GPS System

The GPS receiver *(Global Positioning System)* uses signals with extended spectrum acquired due to direct data signaling, using one of two pseudorandom C/A sequences *(Coarse Acquisition)* and pseudorandom P code, and then phase-modulating both carrier frequencies [15], [16].

Thanks to such application, a significant value of signal to noise ratio S/R *(Signal to Noise Ratio)* is obtained, which, on the other hand, results in a low Bit Error Rate BER *(Bit Error Rate)* as well as increased credibility of the radio transmission.

The figure above (Fig. 5) shows a block diagram containing transmission with widened spectrum using the method of spectrum spreading in DS-SS *(Direct Sequence Spread Spectrum)* systems using code sequences.

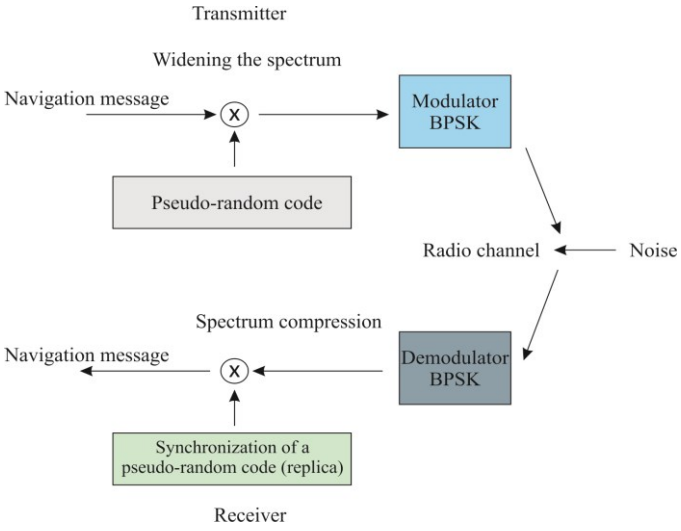

Fig. 5 Block diagram of signal spectrum spreading in a GPS system

Thanks to such application, a significant value of signal to noise ratio S/R *(Signal to Noise Ratio)* is obtained, which, on the other hand, results in a low Bit Error Rate BER *(Bit Error Rate)* as well as increased credibility of the radio transmission [17]. The figure above (Fig. 5) shows a block diagram containing transmission with widened spectrum using the method of spectrum spreading in DS-SS *(Direct Sequence Spread Spectrum)* systems using code sequences.

The main measure of the quality of spreading spectrum systems is the processing benefit *(processing gain)*, determined analogically to the modulation gain included in classical emissions. Information about the processing profit value "G" allows you to determine to what extent the signal to interference ratio has improved at the output S/R_{out} to the ratio of the interference signal at the input of the system S/R_{inp}, therefore:

$$G_{GPS} = \frac{(S/R)_{inp}}{(S/R)_{out}} = \frac{B_{RF}}{B} \quad (1)$$

where:
G_{GPS}- processing profit in GPS,
B_{RF}- the bandwidth of the modulated signal,
B- the bandwidth of the data signal.

A characteristic feature of radio systems with spread spectrum is the increased processing profit. It is generated by spreading the spectrum of the signal, which is then subjected to compression in the GPS receiver. Through this mechanism, only a small element of the radio channel noise is able to productively influence the signal in the GPS receiver.

The advantage of processing in GPS corresponds to the ratio of the bandwidth of the data signal to the modulated signal band. This results in increased noise resistance, which enables the system to function properly despite the signal/noise ratio being reduced [18], [19].

GPS signals with a wide spectrum are obtained by keying data D(t) with a given pseudorandom C/A(t). The bipolar sequence of the pseudo-dependence C/A(t) is multiplied by a bipolar data stream D(t) corresponding to the i-th satellite. T_b (data bit duration) is significantly greater than time $T_{C/A}$ (pseudorandom sequence bit).

The output signal $L_{C/A}$ has a spectrum G-times larger than the data signal D(t). The signal resulting from the modulo-2 sum of both C/A_i(t) and D(t) sequences is transferred to the BPSK phase modulator *(Binary Phase Shift Keying)*, which is transmitted via the satellite to the users. The form of such a radio signal $L_{C/A}$(t) is described by the formula:

$$L_{C/A}(t) = D(t) * C/A_i(t) * cos2\pi f_{L1}t \quad (2)$$

The signal $L_{C/A}(t)$ in the radio channel is affected by interfering factors i(t) of an additive character.

The input signal $L_{C/A}^{inp}$(t) reaches the GPS receiver as the sum of the interference of the form and the useful signal [20].

$$L_{C/A}^{inp}(t) = L_{C/A}(t) + i(t) \quad (3)$$

After completion of the demodulation, the signal is shifted to the baseband in the form of [21], [22], [23]:

$$S(t) = D(t) * C/A_i(t) + i'(t) \quad (4)$$

where: i'(t)- is an interfering signal shifted to the baseband.

In the GPS receiver, the C/$A_i(t)$ code replica is multiplied by the signal *S(t)*, as a result of their synchronization, the course is expressed in the following form:

$$\begin{aligned} S(t) &= [D(t) * C/A_i(t) + i'(t)] * C/A_i(t) \\ &= D(t) * [C/A_i(t)]^2 \\ &+ i'(t) * C/A_i(t) \end{aligned} \quad (5)$$

At the same time after taking into account the identity:

$$[C/A_i(t)]^2 = 1 \quad (6)$$

You get:

$$S(t) = D(t) + i'(t) * C/A_i(t) \quad (7)$$

D(t) is a broadband factor, however i'(t) * C/A_i(t) is a broadband factor. By using a low-pass filter, it is possible to omit almost all of the power of the broadband factor along with the part of the interfering signals, thus allowing receiving a GPS navigational message [24]. The generation of the satellite message is at a speed of 50 [Hz] „a" based on the data transmitted from the control segment, as well as parameters generated via satellite. At the same time, a pseudo-random sequence $C/A_i(t)$ „b" is created - it is different for each of the satellites, having a length of 1023 bit and a generation rate equal to 1.023 [MHz]. Both signals are added modulo 2. Signal „c" of the sum of the message GPS D(t) and the C/A code has a frequency of 1.023 [MHz]. After this process, it undergoes phase modulation [25] (Fig. 6).

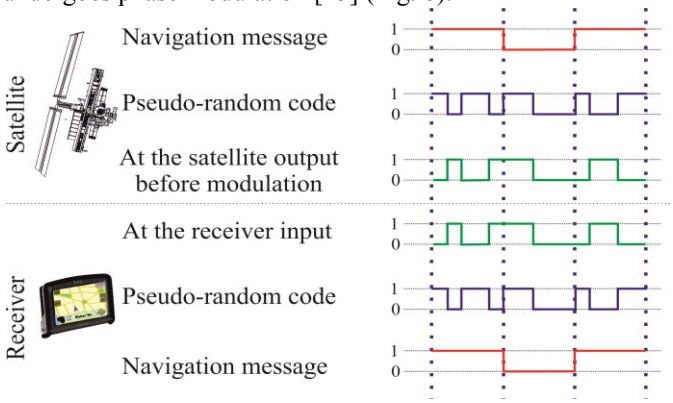

Fig. 6 Transmission of a GPS navigation message

The input signal (d) goes to the user's receiver, where it is added to the C/A code generated by the receiver - replicas (e). At the end, a waveform of 50 [Hz] is obtained, which is a navigational message (f) with the same properties as a message transmitted via satellite (a) [26], [27].

III. The Results of Simulation Studies

To obtain the evaluation of the quality of data transmission, a measurement was made at the transformer output by using the network interference spectrum analyzer (Figs. 7-8) [28].

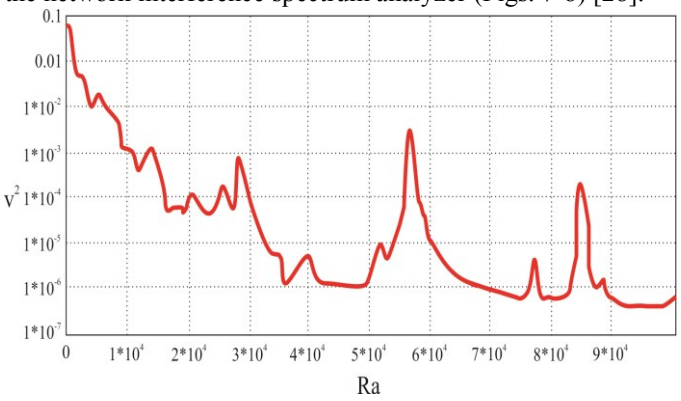

Fig. 7 The spectrum of power interference in the power grid

After conducting and analyzing this measurement, it turns out that the significant share of network interference has pulse power supplies of computers operating in close proximity. This is evident mainly at the lifting frequencies $\approx 58\ [kHz]$ and $\approx 85\ [kHz]$ [29].

To get a measurement of the noise-signal ratio, the power spectrum was measured for two cases:

- during data transmission, where the broadband signal (with interference) has been filtered, and also strengthened,
- in the case of loss of the transmitter signal, where the interference has been amplified and filtered.

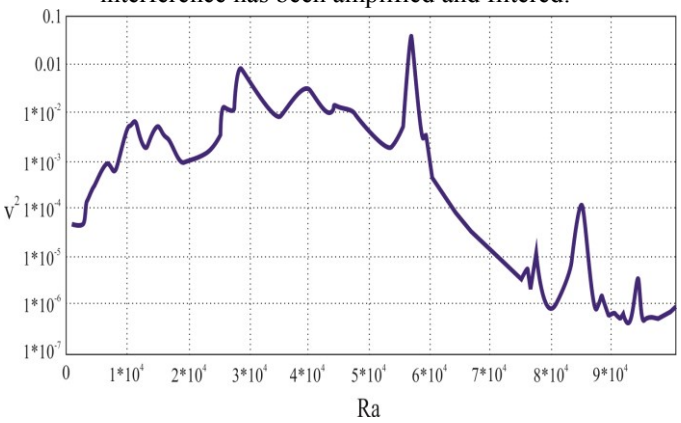

Fig. 8 The power spectrum at the input of the receiver

The result of the calculation of the surface areas under the curves is:

$$\frac{S}{N} \approx 0{,}679 \leftrightarrow -1{,}7\ dB \tag{8}$$

Despite the fact that the power of interference is greater than the power of the useful signal, the correct data transmission was obtained, which confirms the high resistance to interference of systems based on spreading [30].

The developed receiver and transmitter models, although they allow operation (functionality) with signals below a given noise level, have certain limitations resulting mainly from the implemented solutions.

The 255 bit code used can not be called pseudo-random due to its length, so the margin of interference is significantly lower than that resulting from the processing profit.

Based on the experiments conducted, it was concluded that the system is the most sensitive to narrowband interference, of a carrier frequency, which is manifested by distortion of the received data.

TABLE II. Mutual correlation values between code and interference

Sampling frequency 200 [kHz], occupied band 25 - 75 [kHz]				
The code used	Maximum correlation value R_{max}	Interference frequency [kHz]	The correlation value obtained R	Ratio R_{max}/R
[8,4,3,2]	8*255=2040	10	42	48.5
		40	120	17
		50	145	14
[6,5,3,2]	8*63=504	50	68	7.4

Table II shows that the ratio R_{max}/R is significantly smaller than the amount of processing profit G_P, and also depends on the length of the code and the frequency of the interference. Performing tests on the receiver showed that the use of codes smaller than 255 bit is not effective due to the high correlation with interference that occur in the frequency band being used. In addition, for some codes even the correct synchronization can not be received.

IV. The Results of Computer Simulations

It should be noted that the maximum lengths are easy to generate, however, their correlation properties are not good enough to allow them to be used in CDMA (*Code-Division Multiple Access*) systems, using the technique of access to the transmission medium, based on the assignment of individual users using the same channel for data transfer, distraction sequences, thanks to which the receiver will uniquely identify the transmission intended for it.

Gold's sequences and *Kasami's* sequences have much better properties. *Gold* showed that there exist such pairs *u(n)*, *v(n)* *m*- sequences of equal length 2^L-1, for which the function of mutual correlation $R_{uv}(k)$ accepts only three values:

$$R_{uv}(k) \in \{-1, t(L), t(L)-2\} \tag{9}$$

where:

$$t(L) = \begin{cases} 2^{(L+1)/2}+1\ for\ L\ odd\ number \\ 2^{(L+2)/2}+1\ for\ L\ even\ number \end{cases} \tag{10}$$

The sequences *u(n)*, *v(n)* characterized by this property are called the preferred sequences. The values belonging to the set defined are much smaller in terms of the module than the maximum values of the mutual correlation function of any pair

of m-strings that are not the preferred sequences.

Requirements for polynomials that generate preferred strings and tables of their coefficients can be found in the available literature [31].

For example, a short list of selected polynomials defining preferred sequences with lengths N = 31... 2047 is shown in the table III.

TABLE III. Sample pairs of polynomials generating preferred sequences

L	N	Polynomial 1	Polynomial 2
5	*31*	$x^5 + x^2 + 1$	$x^5 + x^4 + x^3 + x^2 + 1$
6	*63*	$x^6 + X^1 + 1$	$x^6 + x^5 + x^2 + x^1 + 1$
7	127	$x^7 + x^3 + 1$	$x^7 + x^3 + x^2 + x^1 + 1$
9	511	$x^9 + x^4 + 1$	$x^9 + x^6 + x^4 + x^3 + 1$
10	1023	$x^{10} + x^3 + 1$	$x^{10} + x^8 + x^3 + x^2 + 1$
11	2047	$X^{11} + x^2 + 1$	$x^{11} + x^8 + x^5 + x^2 + 1$

Gold's sequences are obtained from a pair of m- sequences preferred by the operation of *modulo sum 2* of the first sequence *u(n)* with the cyclic shift of the second sequence *v(n)*. The number of strings obtained in this way is $2^L + 1$ and contains sequences resulting from summing the sequence *u(n)* with $2^L - 1$ possible shifts of the sequence *v(n)* and additionally both *m*- sequences *u(n)*, *v(n)*.

In this way, we get a very large family of *Gold's* sequences with strictly controlled values of the mutual correlation function (number to the first formula from the sub-chapter). For the generation of *Gold's* sequences, a system of two pseudorandom generators is used, using LFSR *(Linear Feedback Shift Register)*, an example of which is shown in Fig. 9. The choice of a specific *Gold's* sequence from an available family is done by setting the initial state of one of the LFSR register generators. Due to the very good correlation properties and the easy selection of a particular family string, Gold's sequences have been used as dissipative sequences in many CDMA systems, such as in the UMTS *(Universal Mobile Telecommunications System)* system or in the GPS satellite navigation system [35].

Kasami's sequences also have very small absolute values of the mutual correlation function. They are obtained similarly to *Gold's* sequences. We distinguish the so-called *a small set* of *Kasami's* sequences containing $2^{L/2}$ binary sequences with the period $N = 2^L - 1$, where *L* is even and so-called *a big set* of *Kasami's* sequences. It also consists of sequences with the period $N = 2^L - 1$, where *L* is even, and contains both *a small set* of *Kasami's* sequences and *Gold's* sequences. In systems with spread spectrum, other sequences are used in addition to those discussed so far, such as OVSF codes *(Orthogonal Variable Spreading Factor Codes)* that act as channel sequences in the UMTS system, or sequences with zero correlation ZCZ *(Zero-Correlation Zone)*, used in LAS-CDMA *(Large Area Synchronous CDMA)* multiple access.

However, due to the small relationship with the subject of this study, they will not be discussed here. In the further part of the work, the results of the computer simulations are presented in the following figures [32], [33], [34] (Figs. 10-19).

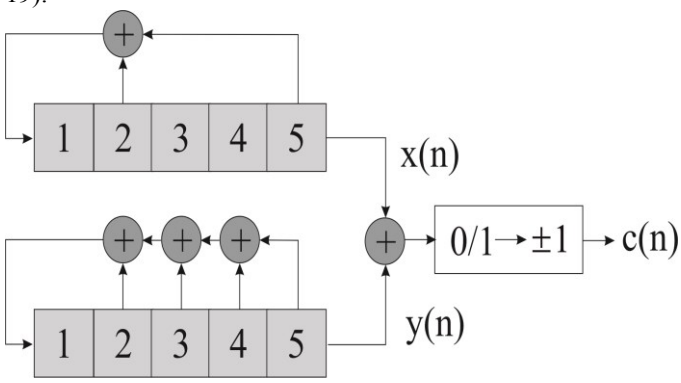

Fig. 9 An exemplary diagram of a pseudo-random generator of *Gold's* sequences

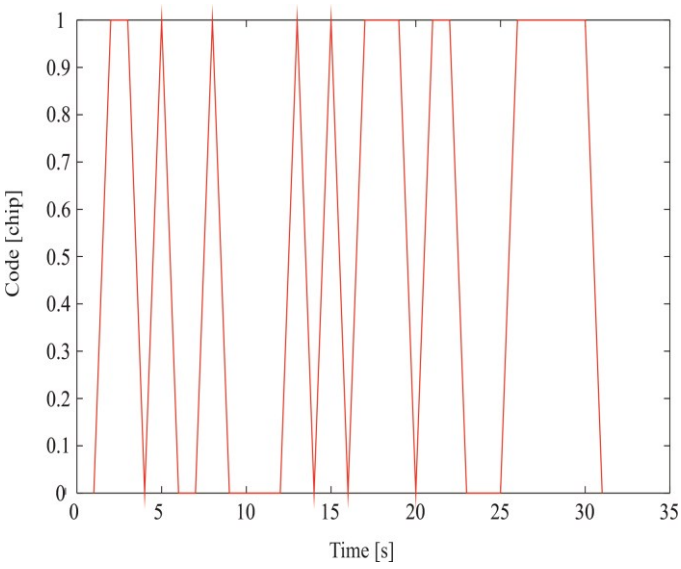

Fig. 10 The pseudo-random code generated by the register No. 1

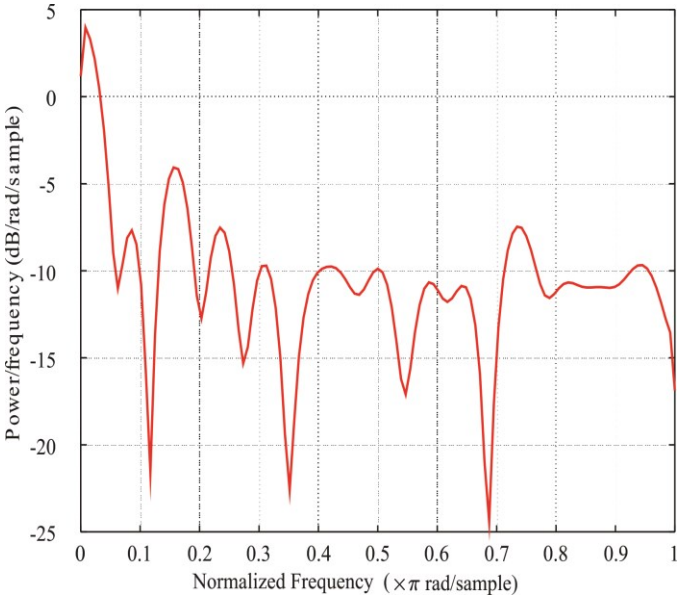

Fig. 11 The spectrum of graph 1 shown in Fig. 10

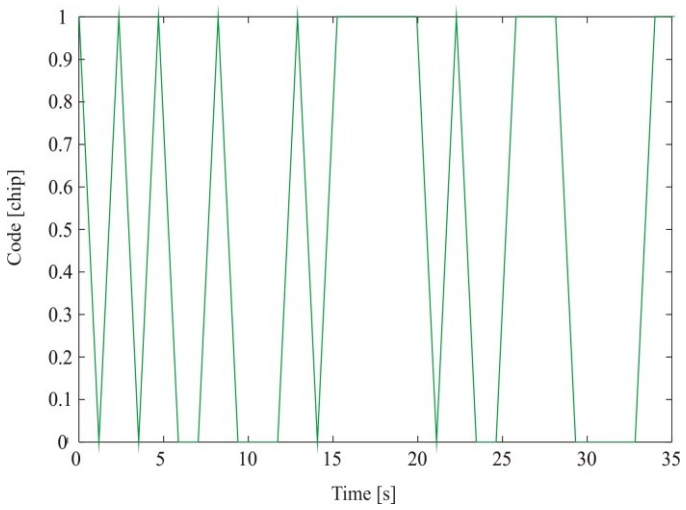

Fig. 12 The pseudo-random code generated by the register No. 2

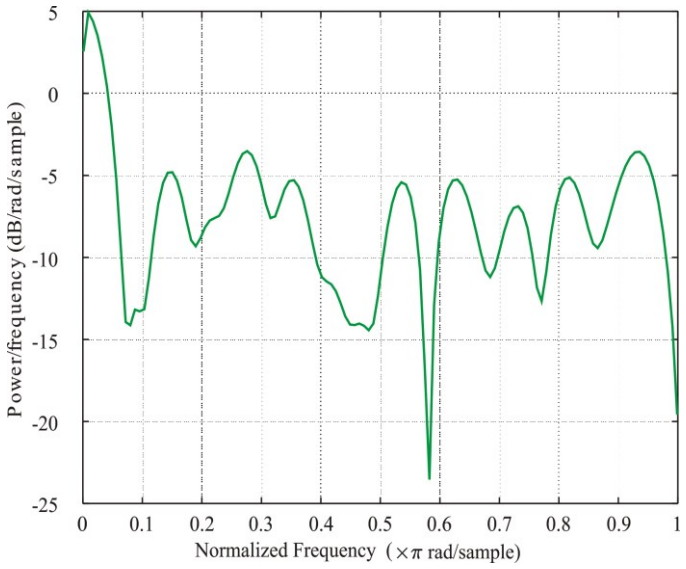

Fig. 13 The spectrum of graph 3 shown in Fig. 12

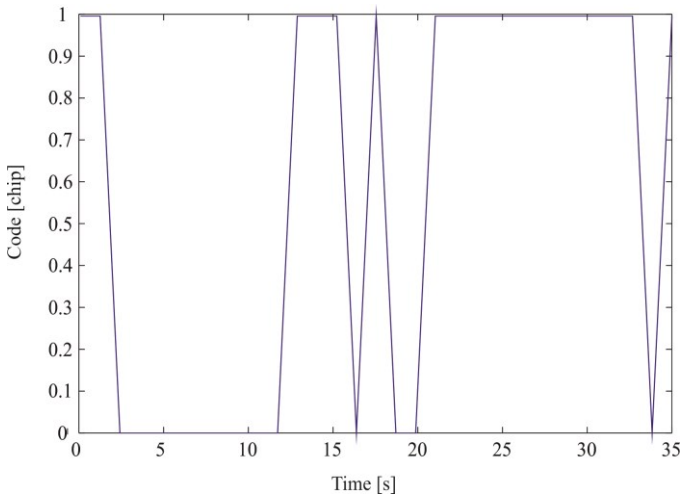

Fig. 14 A pseudo-random code generated by register A

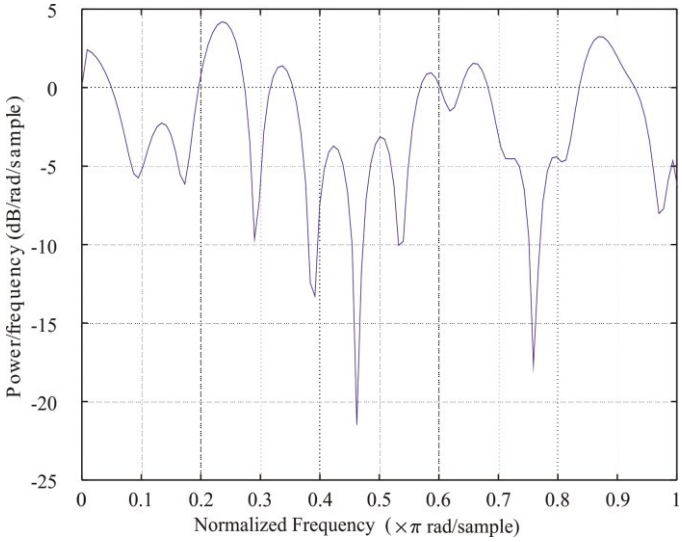

Fig. 15 The spectrum of the graph 5 shown in Fig. 14

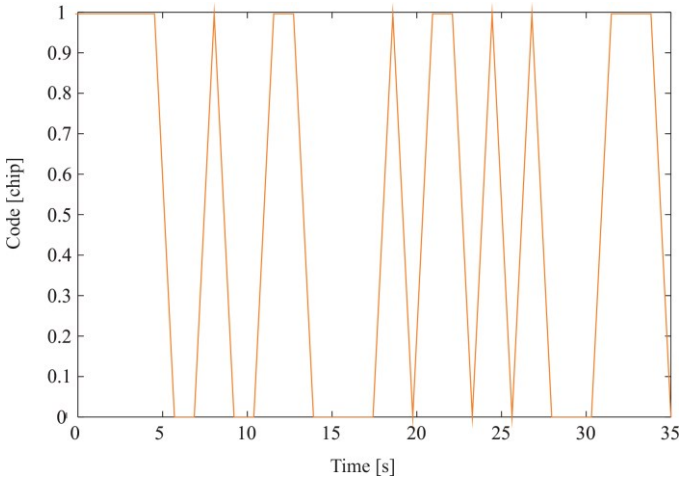

Fig. 16 A pseudo-random code generated by register B

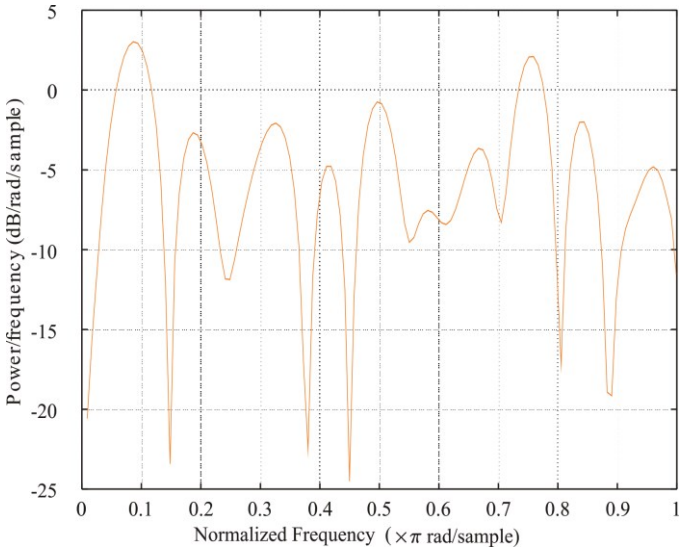

Fig. 17 The spectrum of the graph 7 shown in Fig. 16

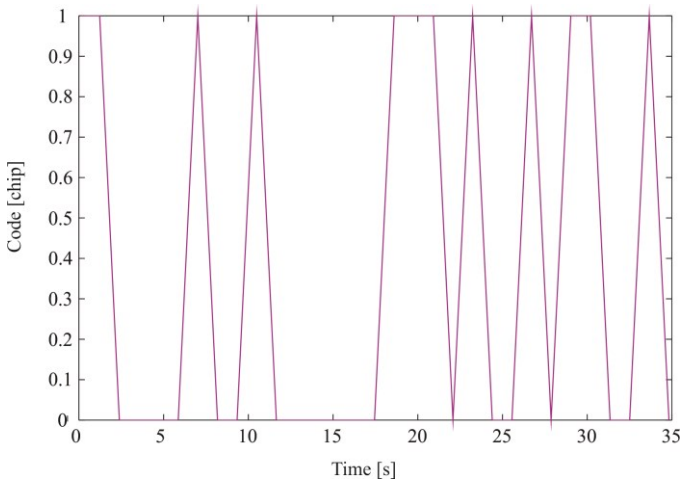

Fig. 18 The pseudo-random code generated by register C

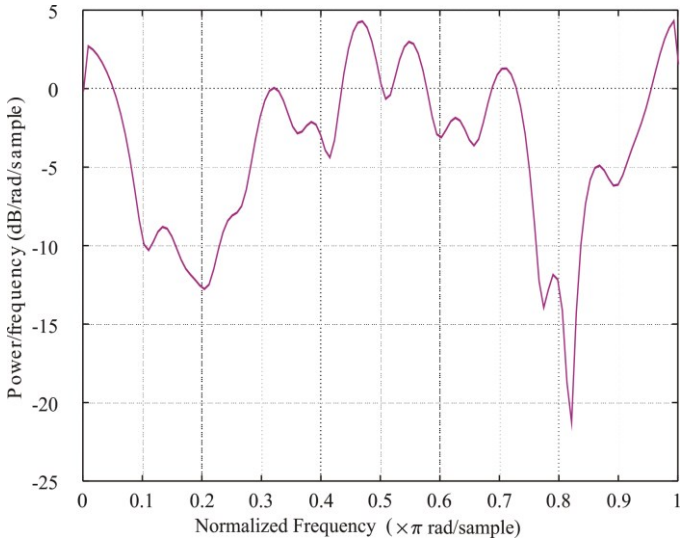

Fig. 19 The spectrum of the graph 9 shown in Fig. 18

V. Conclusion

The pseudo-random codes allow, among others, to carry out measurements to determine the distance between the satellite and the receiver, i.e. the pseudorange necessary to determine the location of a given user. The main task of PRN *(Pseudo Random Noise)* codes is to amplify the signal so that it can be received without the use of parabolic antennas.

In addition, they enable supervision of access to the space segment to its owner. Each satellite is assigned an individual C/A code. Due to the aforementioned autocorrelation feature, it is possible to synchronize the signal in the receiver. This allows decoding the message in the signal, as well as determining the delay that the signal has with respect to the satellite. This delay can be used to determine the position of the satellite at the time of sending the signal and determine the pseudorange to it.

References

[1] G.W. Hein, J. Godet, J-L. Issler, J-C. Martin, R. Lucas, T. Pratt, "The GALILEO frequency structure and signal design," ION GPS sept. 2001.

[2] "European Commission (1999): Galileo – Involving Europe in a New Generation of Satellite Navigation Services," COM (1999). 54, Brussels, 10 February 1999, de Latour. Code tracking performance of PRS and M-code signals. First CNES workshop on GALILEO signals, October 2006.

[3] Solomon W. Golomb and Guang Gong, "Signal Design for Good Correlation," Cambridge University Press, 2005.

[4] G.W. Hein, J. Godet, J-L. Issler, J-C. Martin, P. Ehrard, R. Lucas-Rodriguez, A.R. Pratt, "Galileo Frequency and signal design," GPS world. June 2003.

[5] L. Setlak, R. Kowalik, and M. Smolak, "The Use of a Modified Phase Manipulation Signal to Interfere GNSS Receivers," Proceedings of the 3rd International Conference on Applied Physics, System Science and Computers (APSAC2017), Dubrovnik, Croatia, September 26-28, 2018.

[6] L. Lestarquit, S. Collet, "Tracking Error Correction Algorithm in case of Quasi-Stationary C/A Code Interference," ION GPS sept. 2000.

[7] J-L. Issler, Laurent Lestarquit (CNES), Mark Wilson, Peter Boulton (GSS, now Spirent), "Development of a GNSS2 navigation signal simulator," ION GPS NTM 99.

[8] European Space Agency and Galileo Joint Undertaking, "Galileo Open Service Signal In Space Interference Control Document (OS SIS ICD)," May 23, 2006. Document can be found on-line at: http://www.galileoju.com/page2.cfm

[9] L. Setlak, R. Kowalik, and M. Smolak, "Doppler Delay in Navigation Signals Received by GNSS Receivers," Proceedings of the 3rd International Conference on Applied Physics, System Science and Computers (APSAC2017), Dubrovnik, Croatia, September 26-28, 2018.

[10] J-L. Issler, L. Ries, J-M. Bourgeade, L. Lestarquit, C. Macabiau, "Contribution of ALTBOC to interference mitigation for civil aviation," First CNES workshop on GALILEO signals, October 2006.

[11] Richard Moreno, Norbert Suard, "Ionospheric delay using only L1: validation and application to GPS receiver calibration and to inter-frequency biases estimation (CNES)," ION GPS 1999.

[12] N. Solomon Moise, "Measurements of Radar and DME Emissions at L5," The MITRE Corporation. 4 October 1999.

[13] L. Lestarquit, P-A. Brison, "Signal Choice for Galileo. Compared Performances of Two Candidate Signals," ION GPS sept 1999.

[14] Lo Sherman, Dennis Akos, Thomas Grelier, Alan Chen, Grace Gao, Joel Dantepal, and Jean-luc Issler, "GNSS Album, Images and spectral signatures of the new GNSS signals," Inside GNSS Magazine, June 2006.

[15] M. Ananda, P. Massat, P. Munjal, K. T. Woo, M. Zeitzew, "Second civilian frequency (L5) with WAAS and navigation messages on block IIF satellites (The aerospace corporation)," D. Hanlon (FAA), K. Sandhoo (MITRE corporation), ION GPS 1997.

[16] L. Lestarquit, N. Suard, J-L. Issler, "Determination of the ionospheric error using only L1 frequency GPS receiver (CNES)," ION GPS 1996.

[17] G.W. Hein, J. Godet, J-L. Issler, J-C. Martin, P. Ehrard, R. Lucas-Rodriguez, A. R. Pratt, "Galileo Frequency and signal design," GPS world, June 2003.

[18] J-L. Issler, L. Ries, L. Lestarquit, O. Nouvel, Q. Jeandel, "Spectral measurements of GNSS Satellite Signals Need for wide transmitted bands," ION GPS sept. 2003.

[19] J-P. Diris, M. Brunet, P. Guillemot, J-L. Issler, L. Lestarquit, J. Dantepal, L. Lapierre, C. Zanchi, P. Dumon, T. Tournier, "Performances assessments and measurements on navigation on-board technologies," GNSS 98. Toulouse

[20] B. Eissfeller, G.W. Hein, J. Winkel and Ph. Hartl, "Requirements on the Galileo Signal Structure," Paper presented at the GNSS Symposium 2000, Edinburgh, UK.

[21] J. Barbier, M. Deleuze, J-L. Issler & co-authors, "European complement to GPS: main experimental results," ION GPS sept. 1994.

[22] L. Setlak, and R. Kowalik, "Mathematical modeling and simulation of selected multi-pulse rectifiers, used in "conventional" airplanes and aircrafts consistent with the trend of "MEA/AEA"," Lecture Notes in Electrical Engineering, International Conference on Applied Physics, System Science and Computers APSAC 2017: Applied Physics, System Science and Computers II pp 244-250.

[23] J-L. Issler (CNES), A. Garcia (ESA), "Pseudolite Network for High Altitude Spacecraft Navigation and Synchronization," NAVITECH 2001. first ESA workshop on onboard navigation techniques, 2001.

[24] Spilker et al., "Family of Split Spectrum GPS Civil Signals," ION GPS 98 Conference Proceeding, 1998.

[25] Pratt A.R., and Owen J.I.R., "BOC Modulation Waveforms," Proceedings of the 16th International Technical Meeting of the Satellite

Division of the Institute of Navigation, ION-GPS/GNSS-2003, September 2003, Portland, Oregon, pp. 1044-1057.
[26] L. Ries, L. Lestarquit, J-L. Issler, A.R. Pratt, G. Hein, J. Godet, P. Dondl, F. Couturier, P. Erhard, J.I.R. Owen, R. Lucas-Rodriguez, J-C. Martin, "New investigations on wide band GNSS2 signals L," GNSS 2003, Graz.
[27] L. Setlak, and R. Kowalik, "Analysis, Mathematical Model and Selected Simulation Research of the GNSS Navigation Receiver Correlator," MATEC Web of Conferences, Volume 210, 2018.
[28] M. Ananda, P. Massat, P. Munjal, K.T. Woo, M. Zeitzew, "Second civilian frequency (L5) with WAAS and navigation messages on block IIF satellites," (The aerospace corporation), D. Hanlon (FAA), K. Sandhoo (MITRE corporation). ION GPS 1997.
[29] J-L. Issler, P. Sengenes, J-P. Berthias et al., "DORIS the Next generation. A new and complementary GNSS2 element," ION GPS NTM, January 1998.
[30] J-L. Issler, Laurent Lestarquit (CNES), Mark Wilson, Peter Boulton (GSS, now Spirent), "Development of a GNSS2 navigation signal simulator," ION GPS NTM 99.
[31] L. Lestarquit, N. Suard, J-L. Issler (CNES), "Determination of the ionospheric error using only L1 frequency GPS receiver," ION GPS 1996.
[32] Yannick Ernou, Alain Renard, Estelle Kirby, "ATC Radar Interference Impact on Air Receiver," (Thales Avionics), ITM ION GPS 2003.
[33] L. Setlak, and R. Kowalik, "Studies of 4-rotor unmanned aerial vehicle UAV in the field of control system," MATEC Web of Conferences, Volume 210, 2018.
[34] L. Lestarquit, P-A. Brison, "Signal Choice for Galileo. Compared Performances of Two Candidate Signals," ION GPS sept. 1999.
[35] J. Godet CNES, "GPS/GALILEO Radio Frequency Compatibility Analysis," in support to the European Commission Galileo Architecture Support Team, ION GPS.